

# Estimating Body Shapes From Body Measurements

Margarida Lima

**Abstract**— E-commerce increases every single day, however it is still hard for people to buy clothes online because they have no idea of how they will look. To this end, we present an approach to model an approximation of a human body shape with a given set of body measurements in order to fit virtual clothes. To estimate a new body shape from body measurements we compared two different models that we developed. The first one uses linear transformations and the other uses *PCA* weights to estimate a new shape. Additionally, we selected the minimum number of body measurements required to perform an estimation with a similar shape as the ground truth. We evaluated our approach by comparing our results with estimations, and through visual evaluation via pictures and measurements taken from real people.

**Index Terms**—PCA, Linear Transformation, Body Measurements.

---

## 1 INTRODUCTION

According to Digital Commerce 360 website<sup>1</sup>, online apparel sales accounted for 38.6% of total U.S. apparel sales in 2019 and 100% of the growth in retail clothing sales. E-commerce's share of apparel sales has grown nearly 10 percentage points in the past 3 years, as online apparel sales accounted for 34.0% of total U.S. apparel sales in 2018 and 29.9% in 2017. The percentage of online shopping is increasing year after year, and e-commerce captured an even greater share of apparel sales throughout 2020 due to the coronavirus pandemic. As lockdowns became the new normal, businesses and consumers increasingly went digital, providing and purchasing more goods and services online, raising e-commerce's share of global retail trade from 14% in 2019 to about 17% in 2020 [25]. General e-commerce grew by leaps and bounds during the pandemic by 33.6% in 2020, to a total of nearly \$800 billion. In 2021, online shopping will still expand and accelerate far more than it did before shutdowns and social distancing. In fact, *Emarketer*<sup>2</sup> recently estimated that e-commerce will grow another 13.7% in 2021, reaching \$908 billion [12]. In early 2021, the *EY Future Consumer Index [ey]*, which has surveyed thousands of consumers since the early days of the pandemic, found that 80% of U.S. consumers are still changing the way they shop. Sixty percent are currently visiting brick-and-mortar stores less than before the pandemic, and 43% shop more often online for products they would have previously bought in stores [15]. However, many still prefer to buy clothes in a physical store instead of resorting to e-commerce [2, 30, 1], and one of the reasons is due to the fact that it is impossible to know how a piece of clothing would look when dressed [19, 10]. This is because it is hard to model garments in a realistic way. To consider the fabric's physics, material, and texture, it is required a computational power that most devices do not possess yet. In addition, the amount of data needed in order to produce a realistic result is abysmal, which is monetarily expensive. Especially, data that requires high tech hardware like 3D scans, and several people to scan. The issue aggravates when privacy and ethical concerns are pointed out, specially because this data consists on the realistic shape of people's body including 3D models and/or photographs [13]. Everyday new *deepfake* videos are uploaded to the internet and they are almost impossible to distinguish from reality. The ability of this technology to replace a person with another one likeness in a realistic ways have garnered widespread attention for their uses in celebrity pornographic videos, revenge porn, fake news, hoaxes, and financial fraud [7, 9, 21, 23]. This proposal consists on modeling a human shape based on body measurements manually inserted by the user, and to model an undressed human shape, it is necessary to get

naked examples and therefore it is necessary to scan people wearing the bare minimal amount of clothes - underwear. The acquisition of people that are willing to be scanned under those conditions can be hard, because it can be seen as an invasion of personal space. These are a few reasons on why there aren't more solutions to approach the realistic human body representation problem. We approach this problem by comparing two different models, one only using linear transformations and other using feature extraction, to see which is the best approach to model a new body shape from only body measurements. We also wanted to see if the usage of PCA was useful to map body shape with body measurements. We will use polygon meshes that consist on a collection of vertices, edges, and faces that defines the shape of a three-dimensional object with flat polygonal faces, straight edges, and sharp corners or vertices - polyhedral object. This objects can be explicit once all vertex positions are defined in all axes, or implicit. An implicit surface is the set of zeros of a function of three variables. Implicit means that the equation is not solved for  $x$ ,  $y$  or  $z$ . The usage of implicit surfaces would be valid in this project, however, this kind of surfaces are harder to handle and render, and since our dataset consists of explicit surfaces, it makes sense to use algorithms that apply to them. Therefore, we propose to model realistic 3D triangular meshes - meshes composed of triangular faces - of human bodies considering a set of body measurements, in an attempt to accurately output a polygon mesh with the exact same measures as the ones inserted by the user. Is important to highlight the fact that this proposal will focus on approaching the 3D modeling of a realistic 3D human mesh problem with focus on virtual garment fitting. Thus, it is vital that the body shape is as similar as possible to the original one. There will be two different aspects to evaluate the mesh quality in this proposal: the quality of the produced body shape and the body measurements of the final mesh. The first consists in directly comparing the final mesh with the estimated one by measuring Distance between the correspondent vertices of both meshes. Since we will not scan people to validate our approach, in the tests with real users we will compare the final mesh with the users silhouette extracted from pictures. Thus, at the testing phase, the users will need to manually insert their body measurements as well as an RGB image of themselves wearing minimal clothes. The second one consists on analyzing the body measurements of the final mesh and see how close they are to the original ones.

### 1.1 Project Goals

The goal of this project is to produce a realistic 3D model of a human body that considers a set of standard body measurements, e.g., height, waist, breast, and hips. These measurements are provided by the users, and the system will use them to produce a realistic 3D mesh that represents a human body with the specified measurements. As an extra, we will define what are the minimum body measurements required to produce a mesh with a similar body shape as the original one.

---

<sup>1</sup><https://www.digitalcommerce360.com/>

<sup>2</sup><https://www.emarketer.com/>

## 1.2 Results

To evaluate our approach, we calculated the error of our representation facing the estimated results and see what are the relative errors. We also studied the reliability of the result facing the provided body measures, to see if the new estimated shapes respect those measures or not. An analysis will be made to see what are the minimal measurements required to accurately represent the result facing the estimation. As an extra, we will also visually evaluate the reliability of the mesh inspecting pictures.

Our approach that is able to produce a mesh that respects a set of body measurements manually inserted by the users, it is fundamental that the final mesh contains have similar body measurements as the ones inserted. We also expect that the final mesh contains a body shape similar to the user that inserted the measurements. Finally, an analysis will be performed on how many body measurements are in fact needed in order to represent the maximum amount of information. For instance, it could be useful to use 5 measures (out of 10) if it accurately represented 95% of the information, or by other words it could be beneficial to use less measures if it resulted in a small error percentage.

## 2 RELATED WORK

On this section similar projects to this proposal will be presented and their methodologies discussed. This section will aboard all research done about body deformation techniques that better suit to our needs.

### 2.1 Body Deformation

Body representation has always been a major subject in computer graphics. Until very recently, it has been used almost entirely in the gaming industry, to create characters as realistic as possible. Amaury and Daniel Thalmann describe in [5] that there are two major models that are used to represent the human body: surface models and multilayered models. Both models are composed by a skeleton and a skin representation, which can be a triangular mesh or a set of surface patches. With that, it is possible to add deformation functions to simulate the joint movement to add realism to an avatar's animation. Since that this project mainly focuses on parametric models of the human body, the research was also focused on that direction. In this specific case, the parameters are measurements of an individual's body such as height, length of the legs, arms, etc. Those inputs can be manually inserted by the user [6, 24, 26, 27], or the parameters could be learned from a 3D scanned human mesh dataset [6, 14, 26, 4, 16, 18, 22, 24, 11, 8], a RGB image [14, 22, 31] or even a binary image [11]. Once the system obtains those parameters, the next step is to model the mesh accordingly to those parameters. The modeling of a human body is a hard task to accomplish. Recently there's a lot of work in supervised learning done that involved the 3D scanning of plenty bodies [8, 11, 16, 22] that were later used to estimate a body deformation in a variety of poses [Loper2012BlendSCAPE, 8, 16, 18, 4], or just simply to map an image to a 3D model from a single image [11, 22, 32, 14, 31].

#### 2.1.1 Surface Models

A surface model is either a triangular mesh or a set of surface patches, whose deformation is driven only by the motion of an underlying hierarchical structure or skeleton. This kind of model is still mainly used, especially in the gaming industry, because it is much more computationally cheaper, despite the fact that the results are not considered the best. This subsection is divided into three parts: estimating body measurements as parameters, mesh modeling and deformation and mesh animation. The first part talks about approaches that estimate body measurements by plenty of means, mainly 3D scanned meshes or images, and estimates a 3D mesh that best applies to those values. The second part of this section references used techniques that deform meshes, preferentially respect a set of parameters, or body measurements in this case. The third and final part will identify some approaches proposed to deform 3D meshes with different shapes depending on the body pose. Currently available approaches can be divided into two main categories: feature matching where a system directly regress a 3D geometry from images, and template adaptation where the system deforms a template mesh to respect a set of input parameters.

## Estimating Body Shapes

Non surprisingly, the majority of recent work done in creating parametric avatars has been accomplished using a mesh database derived from 3D scanned bodies of real people. However, this process is expensive because it requires some high-end gear. After scanning the necessary meshes, one of the options is to train a system that either estimates body parameters, where given some input, the system would output the body measurements as parameters to estimate the desired body shape. The usage of neural networks proved to be efficient in this topic. In *PIFuHD* [22] it is used a neural implicit functions for shape representation. In *HS-Nets* [11], the parameters themselves are computed based on images as input, and are used to reconstruct the 3D human shapes by using a statistical human shape model based on *SCAPE* [4]. This model was proposed in 2005 and the shape variation is represented by using *principal component analysis (PCA)* on a set of 3D scans of different people in different poses, which includes a low-dimensional subspace of body shape deformations. In *HS-Nets* however, to learn the global mapping from the data to the parameters, a convolutional neural network (*CNN*) is trained. This *CNN* is trained by feeding the images from different views into the network, however the images are concatenated by a merge layer that performs a max operator over each dimension. However, by outputting a 3D mesh with this system might lead to a wrong human body shape representation by misleading its body measurements. This proposal designs a model that receives body measurements as input and outputs a realistic 3D mesh representation of a human 3D mesh with the measurements as constraints. The same argument is applied to *Detailed Human Depth Network (DHDNet)* [31], where Zhang uses *CNNs* in order to estimate a detailed and completed depth map from a single *RGB* image that contains occlusions of human body. Since information is retrieved from an *RGB* image, there is no certainties that the outputted body representation of the individual in the image respects its body measurements. The estimation of a 3D mesh from an image could be useful to evaluate the project by calculate the differences between the mesh obtained from this proposal and the mesh estimated by the *CNN* model, however that process will not be used because as said previously, this systems do not consider the body measurements of the person in the picture as a parameter.

### Mesh Deformation

After obtaining the desired parameters, that in this case correspond to body measurements, either by estimating those values using machine learning, or by manually inserting them into the system, it is necessary to create a 3D model based on those values. The usage of blend shapes allows an approach without requiring any machine learning technique. Morphing requires a final model shape (target) to be able to morph from the base shape until the desired one. The disadvantage of this kind of process is that it requires a lot of modeling by the developers to have one or more target meshes. One example is *HMR* [14], Zhang builds a standard model to be deformed in three different levels and to recover occluded surface details using the depth information. Both *HMD* [32] and Seo in [24] use blend shapes to update the shape of a model in real time by using an iterative interface. *IntExMa* [26] uses a morphing algorithm to comply with the desired body measurements as input. Morph targets are used to define vectors for the deformation of a defined set of vertices in the complete model. The deformations are made in an automatic iterative process that ends up with a model that fits the desired proportions. Another example is [16] where blend shapes are used not only for body poses but also for animations. *SMPL* [16] is a skinned vertex based model that accurately represents a wide variety of body shapes in natural human poses. This model contains four main elements: a template mesh (*T*), shape blend shapes, pose blend shapes and a pose. A template mesh in a T-pose is used, the output will be this same mesh into a certain given pose, where the body shape depends oh that given pose, e.g. if the pose is being sit the belly would pop out a bit more. Shapes blend shapes consist of offsets applied to *T* in order to represent new body shapes and post dependent shape changes. From training 3D scans

of real people in T-pose, shape blend shapes from different parts of the human body are learned to capture human shape variation using *principal component analysis (PCA)*. This results on the principal modifiers that act on mesh's shapes, or by other words, returns the components that most change in the provided dataset. Learning the human body shape through *PCA* is a strategy used by a lot of projects [6, 4, 16, 18, 24, 8] and it is an effective strategy to learn the variation between different human body shapes, that is why this strategy will be used in this proposal as well to learn the blend shapes that most realistic modify a human 3D mesh. In [6] the data base is clustered and statistically analyzed to capture the tendency of body shape variation, and from that tendency the body shape parameters are extracted. One of the meshes is considered to be the basis of registration, or in other words, the ground truth. The mesh's input body sizes are classified into groups and the parameters (body measurements) of that group are taken into account at the  $R3 \mapsto R3$  transformation that is applied to the base mesh in order to output a new mesh with the desired input measurements. The usage of a ground truth seems wise, because that way exists an initial mesh to work with. Seo in [24], uses a template mesh as well by using a database of 3D scanned meshes from real people, and it is used as examples to correspond a template mesh deformations with the body measurements. In fact, the usage of 2 templates (one male and the other female) could be beneficial to generalize each gender better. A third neutral gender could be used as the average of the entire dataset instead of the average of just one gender. Having this, it is possible to apply transformations (in this case, blend shapes) to that mesh to represent a different body shape.

### Animating Body Meshes

The final part is to add movement to a certain mesh, but more importantly is to know how to represent that mesh in different poses. A realistic animation deforms a mesh depending on the body pose and body shape. A very popular approach to this problem is the usage of regression on joints to increase animation correction and realism. Besides the rest pose template, blend weights, pose-dependent blend shapes, and identity-dependent blend shapes, *SMPL* [16] also contains a regressor from vertices to joint locations. Unlike previous models, the pose-dependent blend shapes are a linear function of the elements of the pose rotation matrices. This simple formulation enables training the entire model from a relatively large number of aligned 3D meshes of different people in different poses. It predicts the joint positions for a given body shape as a function of the mesh vertices. Pose blend shapes are learned from training 3D scans of real individuals in a variety of poses, this captures how real bodies differ from blend skinned bodies, and allows the system to learn how to model body meshes segments (different parts of the body) as pose dependent. Given a pose that is provided to *SMPL*, it computes the near contribution of this blend shape, the correct skinning errors and produce realistic pose dependent deformations. Finally the *SMPL* use of standard blend skinning to transform the deformed template shape into the desired pose.

*STAR* [18], being the evolution of *SMPL*, is 80% smaller because it uses far less parameters by defining per-joint pose correctives and learn the subset of meshes vertices that are influenced by each joint movement. This sparse formulation results in more realistic and general deformations and significantly reduces the number of model parameters to 20%. The system learns shape-dependent pose-corrective blend shapes that depend on both body pose and body mass index (BMI), which was huge compared to *SMPL*, since it factors pose-dependent deformations from body shape while, in reality, people with different shapes deform differently. *STAR* also differs from *SMPL* by being trained with an additional 10000 scans of male and female subjects (being added a neutral gender optimization recently), which improves model generalization. Just like *SMPL*, *STAR* also uses a joint blendshape regressor that allows poses to look realistic. This regressor however, is more compact than the previous one by using a different representation, which contributes to the significative reduction of parameters on *STAR* comparatively to *SMPL*.

The consideration of the pose to deform a mesh is a valuable artifact, however it is not the primal concern of this project. This is a desirable

feature that would allow a more realistic virtual dressing by performing animations that a person would do personally in the dressing room, e.g., sitting, jumping, etc. Therefore we do not consider pose variation in this project.

### 2.1.2 Multi-Layered Models

This kind of model takes into consideration that there are several types of body tissues that behave differently. Therefore, this model will differ from the previous one by adding more layers to it (just like the name suggest). A multilayered model is not just composed by a skeleton and a triangular mesh. It is also composed by some intermediary layers such as muscle and fat layer. Here, the motion due an underlying hierarchical structure or skeleton is also applicable, but instead of being directly from the skeleton to the skin, it passes through two intern layers.

This way, when the skeleton moves, that motion will be reproduced by the muscle layer first, then the fat layer, and finally the skin reproduces the result of them all. In terms of animation, this kind of model produces a much better result than a simple surface model, especially when each layer is modelled accordingly.

*Multi-layer Lattice* [iwamoto2015multilayerlattice] achieve that in a really effective way using voxels. A voxel can be seen as a correspondence of a pixel but in a three-dimensional space, therefore it represents a value on that grid and in this case, that value will identify that specific voxel as bone, muscle, fat or skin. This way, with a mesh as an input, this mechanism was useful to fill the interior and to get separated layers without any extra modeling work.

This procedure was especially interesting for this project because the layer classification was made based on inputs that the user would insert, including bone width and muscle-to-fat ratio, just like it is pretended. It was also possible to define such parameters in a body part level, such that the different parts of the character can behave differently during the simulation. For instance, there are characters that contain more fat in the belly than in the legs. The differentiation between layers is useful for animation purposes, in which a layer behaves accordingly to a certain model. For instance, the fat layer should be much more elastic than the muscle one, since the fatty tissues hang loosely under the action of gravity. This model results in more computational complex but much more realistic animations.

Simulating both muscle and fat layers could add some realism to this project, since it is intended to simulate garments with an avatar. Having both layers reacting to external forces would add realism to the dressing experience, since the avatar would react to the clothes in a more realistic way. For instance, if you have an avatar and two pairs of jeans: one of a small size and another of a large size, the avatar would react differently to both of them. Since the fat layer would be dynamic, the smaller pair would be tighter than the larger one and that would reflect on the avatar by squishing it and deforming its body.

Another approach is to use premodeled parts and adjust them to the inside of the input mesh, what is precisely what Michael Pratscher did on *Outside-In* [20]. In similarity to *Multi-layer Lattice*, *Outside-In* also receives a mesh as an input and the insides are filled, in this specific case, with artificial muscles. The user can then change the muscle sizes in order to give the avatar the desired shape. Contrary to *Multi-layer Lattice*, this project only considers the muscle layer. This kind of approach would definitely add more realism to the virtual mannequin, because each user could customize their avatar in their own way, but since the virtual mannequin should be as realistic as possible, the fat layer should not be ignored.

Despite the fact that a multi-layered model would result in a more realistic outcome, adding a soft tissue layer is a desirable feature for future work and it is not considered on the project. Therefore, it won't be part of the proposal itself, instead it will be on the future work.

## 3 ESTIMATING A NEW SHAPE USING BODY MEASUREMENTS

To approach the problem of estimating a new body shape based on body measurements, our approach is divided in three major sections: preprocessing, model generation, and evaluation. The first step is to preprocess the dataset. In this step, the template models are created, measured, and analyzed in terms of their body measurements and

coordinates. With that information, it is possible to create a mesh of any shape given a set of body measurements as input.

In the first stage, we preprocessed the *Semantic Parametric Reshaping of Human Body Models* [29] dataset to be used in the next steps, and it begins by repairing the meshes. This is an essential step as it prevents any mistake that might happen while extracting the body measurements. After reparation, all meshes will be segmented into sub-meshes, where each submesh represents a different part of the body (torso, upper leg, lower leg, etc). Since the dataset is only composed by meshes, without any kind of landmarks, like height, arm length, leg length, waist, etc, it is necessary to extract those distances ourselves. That was accomplished by using three different distances between points on the mesh: length, height, and girth. The usage of distances like geodesics is important because it takes into consideration the mesh surface to compute Distance. It simulates what a tailor would do while measuring people. The measurements are be useful to learn how different body parts deform, and to apply deformations based on body measurements that users manually insert into the system. After this, the model generation module can initiate.

The learning process is marked by two different models that will be compared with each other. The first one uses feature extraction to learn the principal components that vary in a human body, relate it to the body measurements, and apply the learned model to new sets of body measurements. The other model only uses feature selection to learn which subset of body measurements describe human shape the best. It learns a model for that subset and applies it to any new subset that is inserted. Both models receive body measurements as input that they use to learn how human body shapes vary based on body measurements, and output an entirely new shape based on the inserted measurements.

### 3.1 Preprocessing

The input of the preprocessing module are the meshes of the *Semantic Parametric Reshaping of Human Body Models* [29], and the output are two new datasets computed from the original one: the vertex coordinates of each mesh, and the body measurements of each mesh. We first clean the samples by correcting any geometry imperfection that they might have: internal faces, non-manifold vertices, etc. The preprocessing process continues with the segmentation followed by the creation of the required datasets from the 3D meshes.

#### 3.1.1 Dataset

To extract information about human shape variation, Yipin Yang results in *Semantic Parametric Reshaping of Human Body Models* [29] are used. The dataset is composed of around 3000 meshes, where 1500 are male and 1500 are female. All samples have been placed in point to point correspondence, means that for two meshes  $m_1$  and  $m_2$  all vertices  $v_i \forall i$  in  $V$  are in the same semantic region. Correspondence is established by nonrigid deformation of a template mesh obtained from averaging all female and male meshes (separately). Each mesh contains 12500 vertices and all meshes are positioned in a neutral pose. However, the pose of all meshes is slightly different due to human errors. For instance, if two different people were asked to position themselves in the same position, the final pose would always differ from person to person because of the angle of the arms or even the position of the feet. This means that the dataset is not perfect as it contains pose differences that can compromise the body measurements and the overall results. We do not consider the pose in this project.

#### 3.1.2 Mesh Repair

The software that were used while producing [29] did not consider that the mesh contained non-manifold vertices. We imported a random mesh of the dataset to *Blender*<sup>3</sup> software and an initial evaluation of the mesh showed that it required more fixing than expected. The mesh contained non-manifold vertices on the left foot which could become a problem in later stages as it could interfere with the extraction of body measurements.

<sup>3</sup><https://www.blender.org/>

To solve this problem, it is necessary to repair all meshes of the dataset. Unfortunately, *Blender* is unable to do that, so we needed to use another software to repair the meshes. We used the *Wrap 3*, a paid tool of the company *Russian 3D Scanner*<sup>4</sup>, but since this is a paid tool, we took advantage of the free trial to execute the repairing process. *Wrap 3* solved the non-manifold vertices by adding more vertices to where was an edge shared with more than 2 faces. In the end, the repairing process added 5 more vertices to each mesh, resulting in a repaired dataset where each mesh contained 12505 vertices and no non-manifold vertices.

#### 3.1.3 Extracting Body Measurements

Users will manually insert body measurements as the system's input. The measurements required are split into 3 different categories: *girth* that measures Distance around the middle of something, *length* and *height* that measure Distance between 2 points. The extracted body measurements will be tabled values that are mostly used by the fashion industry, and this measurements are represented in Tables 2, 1 and 3.

The fact that the *Semantic Parametric Reshaping of Human Body Models* dataset [29] is in point correspondence allows to extract body measurements by defining the initial and target points of the distance to measure. Since all meshes are in point correspondence, this information is equal to all meshes.

Height measures the distance between two points using the Euclidean Distance on the  $z$  axis (the vertical one). The length measurement consist on the distance between two points considering the mesh's surface that contains the initial and target points. This type of measurement is useful to calculate the distance between two body parts considering the body shape, just like fashion designers when extracting body measurements from models. Lastly, girth measurements are calculated by intersecting a plane with the mesh to be measured.

## 4 MODEL GENERATION

The preprocessing phase results in a clean selected dataset that can be used to fuel our model to generate new body shapes entirely from a set of body measurements. In this section, we explain how we generate new body shapes from a set of body measurements.

We compare two distinct methodologies against each other, the first simply uses linear transformations to output a new body shape, while the second one uses feature extraction to explain the maximum variance in the human body. However, before we estimate any new body shape, it is fundamental to decrease the number of features that the dataset contains. To fulfill our goal of obtaining the minimum body measurements set that explains as much information as the original set as possible, we perform unsupervised feature selection on the original dataset. In this project, we do not want to classify the gender of a mesh, or the age, we do not have a classification problem in hand. Thus, the usage of supervised methodologies for body measurement selection would be ineffective for this project. The process of feature selection reduces the used features to approximately 17%, resulting in only seven final features of the initial 41. Both of our models use the subset returned from the feature selection process to output new body shapes.

### 4.1 Feature Selection

We first start by selecting the minimum number of features that explain the maximum of the human body variance. We perform feature selection strategies on the original body measurements dataset, to reduce the number of features required to output a new realistic body shape.

Feature selection differs from feature extraction by returning a subset of the original variable set, while feature extraction extracts the principal components of a set and creates an entire new subset featuring those components. This problem is not a classification problem because we do not want to classify a body shape, or gender, or anything, we do not have a target class. That means that observing the human shape is an unsupervised problem and requires an unsupervised feature selection approach. In this project we filter the more important variables by their

<sup>4</sup><https://www.russian3dscanner.com/>

Length		
Measurement Parameter	Definition	
3	<i>Shoulders</i>	The distance between the shoulders following the collarbones.
5	<i>Rise</i>	The distance between the waist passing by the crotch to the back point of the waist.
16	<i>Glutes</i>	The distance between the back point of the abdomen passing by the center of the glute to the beginning of the leg.
17	<i>Neck to Waist</i>	The distance between the center back point of the end of the neck to the back center point of the waist.
18	<i>Collarbone to Waist</i>	The distance between the top point of the collarbone passing by the widest part of the bust to the waist.
20	<i>Upper Arm</i>	The distance between the shoulder to the elbow.
21	<i>Lower Arm</i>	The distance between the elbow to the wrist.
22	<i>Breast</i>	The distance between the top point of the chest passing by the widest part of the bust to the under bust.
25	<i>Front Lower Trunk</i>	The distance between the central point of the waist to the lowest point of the groin.
30	<i>Armpit to Waist</i>	The distance between the lowest point of the armhole to the waist.
31	<i>Collarbone to Under bust</i>	The distance between the collarbone passing by the widest part of the bust to the under bust.
32	<i>Under bust to Belly Button</i>	The distance between the central front point of the under bust to the belly button.
35	<i>Arm</i>	The distance between the shoulder passing by the elbow to the wrist.
37	<i>Groin</i>	The distance between the lowest central point of the abdomen to the lowest point of the groin.
38	<i>Belly</i>	The distance between the lowest central point of the under bust to the lowest central point of the abdomen.

Table 1. Length type measures asked as input by the system. Users will need to measure themselves, it might be required an extra person to help to take the measurements.

Girth		
Measurement Parameter	Definition	
1	<i>Waist</i>	Perimeter of the narrowest part of the torso.
2	<i>Head</i>	Perimeter of the widest part of the head.
4	<i>Bust</i>	Perimeter of the widest part of the bust.
6	<i>Hips</i>	Perimeter of the widest part of the hips.
8	<i>Knee</i>	Perimeter of the widest part of the knee.
9	<i>Ankle</i>	Perimeter of the narrowest part of the ankle.
11	<i>Neck</i>	Perimeter of the narrowest part of the neck.
12	<i>Lower Arm</i>	Perimeter of the widest part of the lower arm.
13	<i>Upper Arm</i>	Perimeter of the narrowest part of the upper arm.
14	<i>Wrist</i>	Perimeter of the narrowest part of the wrist.
16	<i>Tight</i>	Perimeter of the widest part of the tight.
18	<i>Calf</i>	Perimeter of the widest part of the calf.
22	<i>Arm loop Girth</i>	Perimeter of the loop from the top of the shoulder to the armpit.
26	<i>Elbow</i>	Perimeter of the widest part of the elbow.
29	<i>Abdomen</i>	Perimeter of the widest part of the abdomen.
30	<i>Under bust</i>	Perimeter of the widest part of the under bust.
32	<i>Mid Tight</i>	Perimeter of the narrowest part of the mid tight.

Table 2. Girth type measures asked as input by the system. Users will need to measure themselves, it might be required an extra person to help to take the measurements.

Height		
Measurement Parameter	Definition	
7	<i>Waist to Knee</i>	Distance between the waist and the knee.
15	<i>Waist</i>	Distance between the waist and the floor.
17	<i>Inseam</i>	Distance between the lower groin and the ankle.
27	<i>Feet</i>	Distance between the ankle and the floor.
31	<i>Torso</i>	Distance between the neck and the lowest groin point.
36	<i>Neck</i>	Distance between the jaw and the collarbone.
37	<i>Hips to Ankle</i>	Distance between the hip and the ankle.

Table 3. Height type measures asked as input by the system. Users will need to measure themselves, it might be required an extra person to help to take the measurements.

variance and correlation. The usage of the variance in the selection of variables is important because we want to keep the variables that describe better the body shape variation, rather than keeping redundant variables. Correlation is any statistical association, although it commonly refers to the degree to which a pair of variables are linearly related. Thus if two measurements are correlated, we can predict one measurement from the other and vice versa and select only one for the final subset, reducing redundant variables.

The usage of feature selection strategies will be performed on male and female datasets separately. By doing this, we will not only observe how the human body shape varies but also how gender impacts the human body shape.

#### 4.1.1 Data Analysis

The process of unsupervised Feature Selection consists on analyzing the dataset that we want to reduce. Thus, in this section we describe in detail our analysis that lead to the filtering of seven measurements out of 41.

We first checked the amount of missing values on the measurements dataset, but since there were none, we proceeded to the distribution analysis of each variable. We replaced all outliers that were outside of the  $\mu \pm 3\sigma$  Gaussian boundary by missing values, to prevent entropy in our system. The analysis of the missing values count after replacing the outliers indicated that the girth measurements were more affected by missing values than the other measurements, specially the underbust girth, bicep girth, armhole girth and knee girth. Since those measurements were prone to high amounts of error, we decided to exclude them from the final subset. Next, we normalized all variables and then sorted them by variance and plotted it. The normalization step is fundamental, each variable was scaled by shifting their values so that they end up ranging between 0 and 1. This process brings equality to all measurements by being able to directly compare the height with the head girth and see which one changes more overall. To select the final subset of variables, we must select the ones that have a higher variance. This strategy is unsupervised, because we do not contain a target variable in the dataset.

We selected the top 10 body measurements that most vary in both datasets. There are many measurements that both genders share, while there are others that are characteristic of each gender. Selecting 10 variables out of 41 is already a reduction of more than 83% of the original dataset, but we can reduce the final subset even more.

To further decrease the final subset, we need to analyze the relation between the variables, something that can be accomplished by calculating the correlation between the variables. By analyzing the correlation relationship of the top 10 measurements, we concluded that all height measurements are highly correlated. This means that all height mea-

Body Measurements	Gender	
	Male	Female
1	Bust Girth	Bust Girth
2	Hips Girth	Hips Girth
3	Thigh Girth	Abdomen Girth
4	Waist Girth	Thigh Girth
5	Abdomen Girth	Height
6	Height	Waist Girth
7	Neck Girth	Mid-Thigh Girth

Table 4. Final body measurements subset per gender sorted by higher (1) to lower (7) variance. Both subsets have the first 6 elements in common (even with a different sequence) and only the last element of both subsets is unique.

surements can be predicted using only the height measurement. Thus, any other height measurement in the top 10, besides height, can be removed without any information loss. By removing all height measurement, besides the height itself, from the top measurements, the female subset gets with 7 measurements and the male one with 9. In the male dataset, the neck girth is correlated both with the rise and underbust to belly button lengths. This means that the neck girth contains a high percentage of the information that those two measurements contain, and if we delete them, we would still have partial information about them in the neck girth measurement.

At the end of the feature selection process, we ended with 2 subsets of 7 body measurements, as shown in Table 4 with a high level of variation that are not correlated among them. Both subsets share 6 measurements in common, leaving only one measurement that is unique for each gender: neck girth for males and mid-thigh girth for females. We were able to reduce the initial set of measurements by almost 83%.

## 4.2 Estimating New Body Shapes From Body Measurements

After we selected the features that describe the variation of the human body the most, we can implement our models - linear and *PCA* - using that subset. However, the models implemented do not depend directly on the subset used. By other words, the models apply to any body measurement set. This means that the models can be tested using several subsets. Both of these models output a new 3D shape entirely from a set of body measurements.

## 4.3 Estimating New Body Shapes Using *PCA* Weights

In this section, we explain the implementation of one of the two models compared in this project. This particular model will use feature extraction to understand how the human shape dataset, containing vertex positions of all samples, varies.

It is important to understand that the feature extraction process was performed on a different dataset that suffered from the feature selection process. The feature selection is applied on the dataset containing the body measurements, while the feature extraction is performed on the dataset containing the vertex positions of the samples. This means that the feature extraction process is completely independent of the feature selection process. However, in this specific model, we use both processes. The feature extraction is performed on the coordinates dataset using Principal Component Analysis (*PCA*). This results in the model learning the principal components of the dataset. These principal components represent how the human shape varies the most, with each component representing a specific body variation e.g, the height, the breast size, the body volume, etc. These principal components are mapped as weights and are associated with the vertices of a template mesh obtained from the mean of the samples used to train our model. The template model is deformed by adding the weights associated with the new set of body measurements. Finally, once we insert a new set of body measurements, the model outputs a new body shape that respects the body measurements inserted.

### 4.3.1 Feature Extraction Algorithm

The first step of this model is to calculate the template models  $\bar{S}$  for male and female genders. These templates consist on the mean of all male and female meshes in the dataset, respectively. It is of the most importance to calculate the template meshes because it will be the foundation of this model.

This approach is accomplished by extracting information regarding the vertex coordinates of the samples and is based on S. Wuhrer proposal for estimating human shapes based of body measurements [28]. As input to the method, it is given a database of  $n$  triangular manifold meshes  $S_0, \dots, S_{n-1}$  of human bodies with similar posture and a set of measurements  $P$ . Let  $P_i$  denote the measurements corresponding to  $S_i$ . Furthermore, we are given a set of distances  $P_{new}$ . Our aim is to estimate a shape  $S_{new}$  that interpolates the distances  $P_{new}$ . This approach proceeds by learning the correlation between the shapes and the measurements.

The template meshes  $\bar{S}$  are used to calculate how much the samples differ from the average shape. Therefore, there is a new dataset  $D$  that is composed by the differences between all samples of  $S$  and  $\bar{S}$ , as it is demonstrated in Equation 1.

$$D = S_i - \bar{S}, \forall S_i \in S \quad (1)$$

Let  $D$  be a  $(3v \times n)$  matrix, by performing *PCA* in  $D$ , it yields a matrix  $y$  that corresponds to the transformed dataset  $D$  and a matrix  $A$  that is a transformation matrix. The first matrix  $W$  and matrix  $D$  are the representation of the same information but in different spaces. By applying *PCA* to  $D$  we extract the information in the dataset by creating a new coordinates system that fits the data where it varies the most. In other words, we lose information regarding the variables of  $D$  because new ones are created. The second matrix  $A$  is the matrix that allows the transformation of  $D$  into  $W$  and vice versa, it is a transformation function. Thus, a new shape  $S_{new}$  can be estimated using the Equation 2 where the sum of the template mesh  $\bar{S}$  and the weights of a new set of measurements  $W_{new}$  transformed by  $A$  result in a new shape  $S_{new}$ .

$$X_{new} = AW_{new} + \mu \quad (2)$$

However we still need to calculate matrices  $A$  and  $W_{new}$ . We know that  $W$  is  $D$  transformed into the *PCA* coordinate system, thus a transformation  $A$  is responsible for the coordinate system swapping. So,  $W$  is the result of the multiplication of  $A$  and  $D$ , what means that we can obtain  $A$  by multiplying  $W$  and  $D$ , like demonstrated in Equation 3 with  $D^+$  being the pseudo-inverse of  $D$ .

$$W = AD \Leftrightarrow WD^+ = ADD^+ \Leftrightarrow WD^+ = AI \Leftrightarrow A = WD^+ \quad (3)$$

To calculate the weights matrix  $W_{new}$ , we need to take into consideration the body measurements and relate them to the *PCA* weight  $W_i$  of each mesh  $S_i$ . For that, we learn a linear mapping from  $P_i$  to  $W_i$  with  $i = 0, \dots, n - 1$ , by transforming each  $P_i$  to a new coordinate system  $W_i$ . To perform this, we need another transformation matrix  $B$  that maps body measurements to its corresponding *PCA* weight. We can infer  $B$  by assuming that  $W_i$  is the result of the multiplication between  $B$  and  $P_i$ , like demonstrated in Equation 4, with  $P^+$  being the pseudo-inverse of  $P$ .

$$W = BP \Leftrightarrow WP^+ = BPP^+ \Leftrightarrow WP^+ = BI \Leftrightarrow B = WP^+ \quad (4)$$

With this, we are able to relate the body measurements to the information extracted from the human body variation through *PCA* and give it a weight. It is important to notice that to reproduce the results obtained in [28] we must normalize each entry of  $W$  by its correspondent *PCA* eigenvalue. Finally, to estimate a new shape  $X_{new}$  based on a new set of body measurements  $P_{new}$ , we can transform  $P_{new}$  to the *PCA* coordinates, resulting in a weight vector  $W_{new}$  and then transforming  $W_{new}$  to the coordinate system that dictates the shapes. Therefore, we can re-write the Equation 2 into Equation 5.

$$X_{new} = ABP_{new} + \mu \quad (5)$$

The mapping between the measurements and the PCA weights of the 3D shapes learned allows us to find a new shape  $S_{new}$  new given  $P_{new}$ . With this process we can understand how much the human shapes vary from the average human shape  $\bar{S}$ . We can relate that variation with the body measurements  $P$  and estimate new shapes  $S_{new}$  with a new set of body measurements  $P_{new}$ . By adding the weights corresponding to a new set of body measurements  $W_{new}$  to the template mesh  $\bar{S}$  we obtain a new shape that respects the variation dictated by  $P_{new}$ .

#### 4.4 Estimating New Body Shapes Using Linear Transformations

This second model obtains a shape directly from the body measurements. We accomplish this by creating a transformation matrix between the coordinates and body measurements datasets. This way, we can easily transform a body measures vector into a coordinates vector without intermediate steps.

#### 4.5 Linear Transformations Algorithm

Let  $S$  be coordinates dataset and  $M$  be the body measurements dataset. Both datasets contain  $k$  samples, because they both have different information regarding the same 3D objects. Each sample contains  $3v$  vertices and  $m$  body measurements. Lets assume that there is a function  $T$  that maps a vector of body measurements  $M$  into a vector of vertices coordinates  $V$ , as shown in Equation 6.

$$T : M \rightarrow V \quad (6)$$

In this case,  $T$  represents a linear transformation mapping the space of body measurements to the space of 3D coordinates. So,  $T$  is a linear transformation mapping  $\mathcal{R}^m \rightarrow \mathcal{R}^{3v}$  and given a column vector  $x$  with  $m$  entries then the transformation function can be represented as in Equation 7, where  $T(x)$  returns a column vector with  $3v$  elements.

$$T(x) = Ax \quad (7)$$

For  $T(x)$  return a column vector with  $3v$  elements,  $A$  must be a  $(3v \times m)$  matrix. Note that  $A$  have  $3v$  rows and  $m$  columns, whereas the transformation  $T$  is from  $\mathcal{R}^m$  to  $\mathcal{R}^{3v}$ . This follows the linear algebra rule that for matrix multiplication to happen, the number of columns in the first matrix must be equal to the number of rows in the second matrix. The resulting matrix has the number of rows of the first and the number of columns of the second matrix. With  $A$  being a  $(3v \times m)$  matrix and  $x$  being a  $(m \times 1)$  vector, the  $Ax$  multiplication results in a  $(3v \times 1)$  matrix.

To calculate the transformation matrix  $A$  we just need to start from Equation 7 and isolate  $A$ , just as demonstrated in Equation 7.

$$T(x) = Ax \Rightarrow y = Ax \Leftrightarrow yx^+ = Ax^+ \Leftrightarrow yx^+ = AI \Leftrightarrow yx^+ = A \Leftrightarrow A = yx^+ \quad (8)$$

According to Equation 8,  $A$  can be calculated by calculating the *dot* product between the samples coordinates ( $y$ ) and the pseudo inverse of the body measurements ( $x$ ).

After calculating  $A$ , we are able to map a vector of body measurements into a vector of coordinates with Equation 7. However, the result of that equation is a vector with  $3v$  elements, 3 times more than the sample vertices, because while building the coordinates dataset we joined all vertices coordinates to form a 1-dimensional array. To represent a 3D shape from  $T(x)$  we just need to group the elements 3 by 3, resulting in a set of  $v$  3D points.

## 5 EXPERIMENTAL EVALUATION

Our evaluation process is composed by two main processes: validation and evaluation itself. The validation process is intended to verify that models are performing as expected. As an extra, we observed which model performed the best and used the winner to the final evaluation process that involved real users. The validation and evaluation process

are qualitatively evaluated based on the estimations body shape and measurements. The estimated body measurements were expressed in centimeters and were directly compared to the original ones in both processes. The qualitatively evaluation of the body shape was compared to the original meshes in validation step and with real users silhouettes in evaluation step.

For the evaluation process, we used six different friends and family members. Unfortunately, we were not able to have a balanced testing sample regarding the gender. We tested five females and only one male. The age ranges of the tested people is in between 21 and 46 years, with the average being 23 years.

### 5.1 Validation

To first validate our approach before testing with real human users, we decided to test our model with four different samples from the database. There are two male and two female scans with one having a smaller size and the other with a bigger size. The usage of samples that cover all spectrum of human shape is important to see if the models know how to deal with all cases.

#### 5.1.1 Body Shape

The validation is made by comparing the shape returned by the model with the original one by measuring the distance between the point-to-point correspondent vertices. In other words, we compare the position of the vertices with the same index on the both shapes and calculate the Euclidean distance between them. With all distances calculated, we can visualize the error using a color map, like represented in Figures 2 and 1. Each column represents a different subset, and therefore a different estimation. From right to left in Figures 2 and 1: top 2, top 4, top 6, top 8, top 10, selected 6, selected 7 and ground truth. To validate our linear and *PCA* models, we estimated the same shape using 7 different body measurement subsets: top ten to top two measurements, the best seven, obtained from feature selection, and the selected six, that is composed of only the measurements that both genders have in common in the best seven subset. To address to a specific estimation we will use the nomenclature  $(xy)$  where  $x$  is the row number and  $y$  the column. Therefore estimation  $(3c)$  corresponds to the one on the third row and column  $c$ , that represents the result of the estimation using the top six measurements that vary the most.

In both Figures 2 and 1, we can understand that some body measurements configurations work better than others. We can see that the results are often better when using more measurements. This is supported by the *MSE* values, since they are higher as the number of measurements used to estimate a new shape increases. However, in Figure 2 we see that the difference between  $(1d)$  and  $(1e)$  is almost 0 and their *MSE* difference is of about 0.0002. This indicates that the insertion of the body measurements 9 and 10 is irrelevant, and we can obtain the same results using only the first eight measurements. In  $(1c)$  of Figure 2 we notice a big difference in the height comparing the original sample. This happens specially to male meshes because the height is not part of the top six measurements, however it is more noticeable in  $(1c)$  than in  $(2c)$ . This happens because of the high values of the remaining measurements, like waist bust, abdomen, etc. Like sample *SPRING306*'s body measurements are way higher than average on the dataset and there are not many samples with bigger sizes, the model estimates a new shape using the information that it has. This results in a shape that is very similar to the average male body, but in a bigger scale. This explains why in  $(1b)$  and  $(1c)$  of Figure 1 have a higher distance difference of sample *SPRING0306* in their feet and head, since the center of all meshes is on their groin. To produce a shape with such big measurements, the model scales the shape in order to respect them and the model ends up being huge because in top 6 measurements we do not have height as a constraint. This effect is also visible in  $(1b)$  regarding the top 4 measurements, however in  $(1a)$  it is not visible. It is visible that in  $(1a)$ ,  $(1b)$  and  $(1c)$  the main differences regarding the original mesh are in the belly. Sample *SPRING0306*  $(1g)$  is characterized by having larger dimensions and our linear model may have difficulties representing those dimensions to perfection. However it is able to return a shape with larger dimensions but not as big as the





Fig. 1. Error color map of the pca model using several body measurements sets. Each column corresponds to a subset of the top ten body measurements or from the selected seven from Table 4, from left to right: (a) top two (b) top four (c) top six (d) top eight (e) top ten (f) selected six (g) selected seven (h) original shape. The yellow parts correspond to the parts that have a higher distance error in cm associated, while the dark blue parts are the ones that are more similar to the original shape.

ones inserted. This may be happening because groups of male with larger dimensions are poorly represented in the *Semantic Parametric Reshaping of Human Body Models* dataset [29]. The estimation represented in (1a) is very similar to the ones of columns (1d) and (1e), it even has a similar maximum error (15cm) but it fails to represent the belly in a more similar way. We expected the columns (1g) and (1g) to perform better since the subsets are composed by body measurements that were obtained through feature selection, represented in Table 4. But the absence of the measurements like rise length and/or under-bust to belly button had a negative impact on the returned shape, especially on the belly of the estimations were they have a higher distance error. By analyzing the results of the estimation of sample *SPRING0306* and its MSE values, we conclude that the best subset of body measurements is the top 8.

### 5.1.2 Body Measurements

In this section, we explain how we validate the body measurements with the estimations returned by our models. The validation is made by comparing the body measurements extracted from the estimated shapes with the original ones. The body measurement extraction of the estimated shapes was made just like the extraction of the measurements of the original shape was made to preserve consistency among tests. By observing the results obtained from the estimated body measurements,

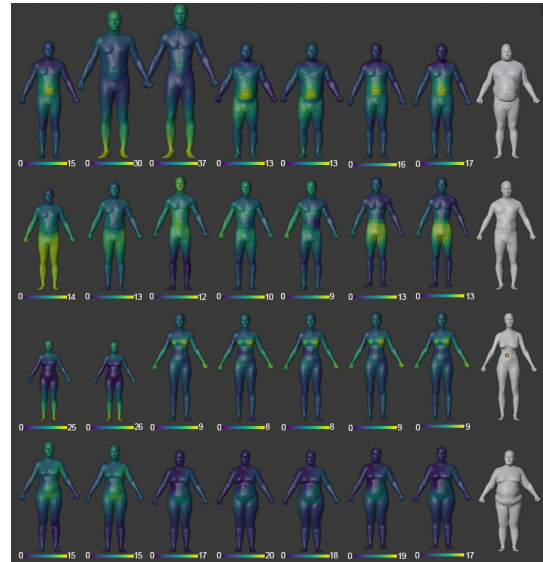


Fig. 2. Error color map of the linear model using several body measurements sets. Each column corresponds to a subset of the top ten body measurements or from the selected seven from Table 4, from left to right: (a) top two (b) top four (c) top six (d) top eight (e) top ten (f) selected six (g) selected seven (h) original shape. The yellow parts correspond to the parts that have a higher distance error in cm associated, while the dark blue parts are the ones that are more similar to the original shape.

we observe that our linear model is more able to estimate shapes that belong to a group that is well represented in the dataset better than samples that are poorly represented. Which means that the estimated measurements of average shapes were more similar to the original ones. In one of the female estimations we could observe that all subsets, except for top 4 and top 2, performed relatively well with a bigger error rate on the girth measurements. Thus, since the usage of the subsets obtained from Table 4 do not produce better results, we will discard them for the evaluation, only focusing on the subsets of the top 10 measurements.

## 5.2 Evaluation

The final and most important part of the evaluation is evaluation step itself - test our model with real users. In this section we will explain how the evaluation with real users was made. We concluded that our pca model was unable to estimate new realistic body shapes given s subset of body measurements. For this reason the linear model was selected as the best performing model and the pca one was excluded. Then, we performed the evaluation process using only the linear model. Therefore, we evaluated our model that uses linear transformations with real people. We tested six different people to validate our model. They were friends and family, with five females and only one male individual. The age ranges of the tested people were between 21 and 46 years, with the average being 23 years. To perform the tests we asked each individual to extract ten body measurements according to top 10 measurements and to take two full body picture of themselves: a frontal and a profile one. Since we did not extract the measurements ourselves, and didn't take the pictures either, we noticed that the action of the individuals to measure themselves is quite complex and difficult. The same can be applied to the photos, we asked for photos at the hip level, however there were some differences in the angle that the pictures were taken. We then used the photos to compare the estimated mesh with the users body shape. We extracted the body measurements of the estimated mesh and compare them to the original ones.

## 5.3 Body Shape

To evaluate our model regarding the estimation of real users body shape, we took two pictures of the users: a frontal and a profile one. Since we



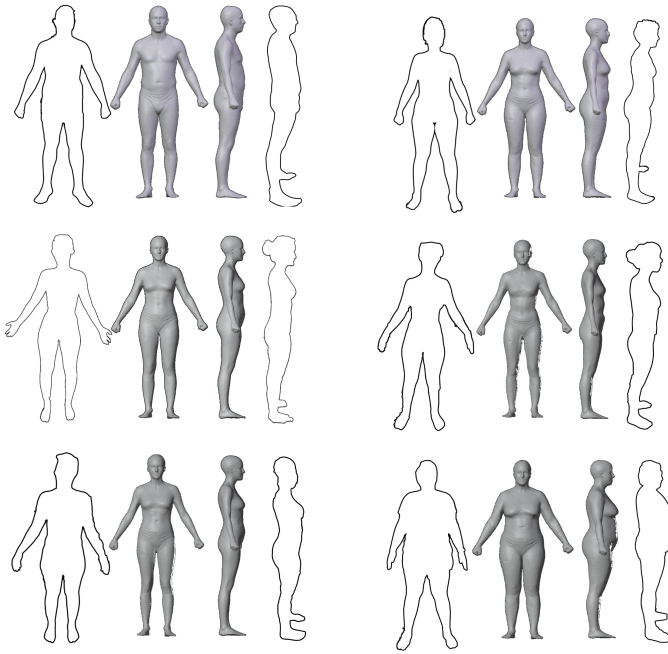


Fig. 3. Visual comparison of real users silhouette with their correspondent shape estimation using the top 8 measurements subset. From left to right and top to bottom we called these estimations  $P_1$ ,  $P_2$ ,  $P_3$ ,  $P_4$ ,  $P_5$  and  $P_6$ .

deal with sensible information on this project, we wanted to protect our testers identification. We did this by only using the silhouettes of their body shape, instead of the raw pictures. First of all, we took pictures of the testers body. Then, we contoured the silhouettes by using *Adobe Photoshop* and removed the filling of the images, resulting only the silhouettes of the users. These images were placed side by side on their body estimation meshes, in Figure 3 we can see the final results.

We noticed that our model has difficulty on model the waist of estimations. In cases where the original shape has hips relatively larger than the waist, as  $P_3$  does, our model returns a shape with a larger waist than it should. However our model estimates shapes with a waist relatively similar to the hips as having smaller waists. Almost every users are considered to be part of the group that is well represented in the dataset: A more slim appearance for both represented genders, and for females a waist that is thinner than the hip. This made possible for our model to return better estimations regarding  $P_1$ ,  $P_2$ ,  $P_3$ ,  $P_4$  and  $P_5$ . Since  $P_6$  belongs to a group that is poorly represented in the dataset, the model struggled to estimate its shape based only in measurements. Besides the waist, our model also had difficulties on estimating fuller thighs.  $P_2$  is a good example, we see that the frontal silhouette (the first image counting from the right of  $P_2$ ) has fuller thighs, something that the estimation does not. It has an indication of fuller external thighs, however the interior of the thighs is not very similar. The estimations presented in Figure 3 are not perfect representations of the users silhouettes, the model had difficulties on correctly estimate waists and thighs. However the estimation returned new shapes that are pretty similar to the original ones. We asked the users if the estimation was similar to their bodies, they pointed some issues like the waist and thighs but said that overall it looked like them. We conclude that our model is capable of estimate a new body shape according to a small set of body measurements input.

#### 5.4 Body Measurements

After evaluating the body shape of our estimations using the linear model, we evaluated the body measurements of the estimations and compared them with the original ones. The first thing that we noticed is that, the estimated height and waist height measurements in female estimations were the same as the original ones. This means that these

measurements did not have any kind of error, and that the visible difference in height in Figure 3 was caused by the perspective and nothing else. However, the inseam height and hips to ankle height measurements had some errors associated. In inseam height, the estimation was off by 12cm in some cases. We realized that this is because people found it difficult to understand how they should measure the inseam height, therefore all users measured it differently. On other hand, our only male sample showed some errors associated with the height measurements, especially in the waist height one. We do not have test samples to support this, but we believe that is because of the fluctuation of the waist point in the dataset meshes. This vertex will always be part of the belly, but depending on the dimensions of the mesh, the vertex might be positioned below or above the waist line, which can lead to errors. The measurement that had more error associated was abdomen girth, with a distance difference reaching up to 31cm. We believe that this is also because the vertex fluctuations on the meshes, and the girth extracted might sometimes be more similar to the waist than the abdomen itself. The estimations of the bust girth are usually smaller than the original one, reaching a distance difference of 5cm in the worst case. We observed that some measurements not behave like this: thigh girth and mid-thigh girth estimations had a higher measurement value than the original one.

Total distance error ( $TDE$ ) is the sum of all distance errors between the original ( $T$ ) and estimated ( $E$ ) measurements. This value helps us understand which body shapes our model struggles more (or less) to estimate according to a measurement constraint. The  $TDE$  per user is  $TDE_{P_1} = 36cm$ ,  $TDE_{P_2} = 66cm$ ,  $TDE_{P_3} = 61cm$ ,  $TDE_{P_4} = 84cm$ ,  $TDE_{P_5} = 51cm$  and  $TDE_{P_6} = 27cm$ .  $P_6$  is the shape with less  $TDE$  given it is the shape that differs the most from the original one according to Figure 3, with an estimated waist far thinner than the original one. According to the results, our model estimated more accurately the new shape measurements that have higher dimensions, but in this case the body shape is far different from the original one. The opposite also applied, more thinner shapes originated estimations that have a similar body shape but with a high  $TDE$  value, normally estimating measurements that are way smaller.

## 6 CONCLUSIONS

Our approach involved the comparison of the two models, one using  $PCA$  weights and the other using linear transformations to estimate new shapes. The comparison of both models was also useful to conclude that the usage of  $PCA$  weights is not appropriate to the estimation of new shapes, thus we only evaluated our linear model.

We evaluated our linear model using the top 8 measurements subset. Just like in the validation step, we evaluated the estimations regarding the estimated body shape and measurements and reached the conclusion that our model is not appropriate to estimate new shapes with similar body measurements as the original shape. And since this project is targeted for a virtual dressing room, it brings concerns on how similar the estimation is to the real user if both the estimation and user do not have the same measurements. Instead of helping the user on choosing a size, it may mislead the user into buying the wrong size. On the other side, our model was able to provide new body shapes that were very similar to the original ones. This was also supported by the users, because the majority said that the estimation had a similar shape as them.

## REFERENCES

- [1] *5 reasons why customers prefer to shop in-store instead of online*. URL: <https://www.collectique.eu/en/5-reasons-why-customers-prefer-to-shop-in-store-instead-of-online/>.
- [2] Gina Acosta. *Consumers Still Prefer Physical Stores*. Oct. 2019. URL: <https://progressivegrocer.com/consumers-still-prefer-physical-stores>.

- [3] Brett Allen, Brian Curless, and Zoran Popovic. "The Space of Human Body Shapes: Reconstruction and Parameterization from Range Scans". In: *ACM Trans. Graph.* 22 (July 2003), pp. 587–594. DOI: 10.1145/1201775.882311.
- [4] Dragomir Anguelov et al. "SCAPE: Shape Completion and Animation of People". In: *ACM SIGGRAPH 2005 Papers*. SIGGRAPH '05. Los Angeles, California: Association for Computing Machinery, 2005, pp. 408–416. ISBN: 9781450378253. DOI: 10.1145/1186822.1073207. URL: <https://doi.org/10.1145/1186822.1073207>.
- [5] Amaury Aubel and Daniel Thalmann. "Realistic Deformation of Human Body Shapes". In: *Computer Animation and Simulation 2000*. Ed. by Nadia Magnenat-Thalmann, Daniel Thalmann, and Bruno Araldi. Vienna: Springer Vienna, 2000, pp. 125–135. ISBN: 978-3-7091-6344-3.
- [6] Seung-Yeob Baek and Kunwoo Lee. "Parametric human body shape modeling framework for human-centered product design". In: *Computer-Aided Design* 44.1 (2012). Digital Human Modeling in Product Design, pp. 56–67. ISSN: 0010-4485. DOI: <https://doi.org/10.1016/j.cad.2010.12.006>. URL: <http://www.sciencedirect.com/science/article/pii/S0010448510002289>.
- [7] ALEC BANKS. *OP-ED — DEEPFAKES WHY THE FUTURE OF PORN IS TERRIFYING*. 2018. URL: <https://www.highsnobiety.com/p/what-are-deepfakes-ai-porn/>.
- [8] Yin Chen et al. "Parametric 3D modeling of a symmetric human body". In: *Computers Graphics* 81 (2019), pp. 52–60. ISSN: 0097-8493. DOI: <https://doi.org/10.1016/j.cag.2019.03.013>. URL: <http://www.sciencedirect.com/science/article/pii/S0097849319300366>.
- [9] Jon Christian. *Experts fear face swapping tech could start an international showdown*. Feb. 2018. URL: <https://theoutline.com/post/3179/deepfake-videos-are-freaking-experts-out>.
- [10] Terry Clark. *Benefits of Physical Store vs Online Shop*. Mar. 2020. URL: <https://retail-focus.co.uk/benefits-of-physical-store-vs-online-shop/>.
- [11] E. Dibra et al. "HS-Nets: Estimating Human Body Shape from Silhouettes with Convolutional Neural Networks". In: *2016 Fourth International Conference on 3D Vision (3DV)*. 2016, pp. 108–117. DOI: 10.1109/3DV.2016.19.
- [12] Sharon Goldman. "Post-pandemic e-commerce: The unstoppable growth of online shopping". In: Aug. 2021. URL: <https://www.the-future-of-commerce.com/2021/08/03/post-pandemic-e-commerce/>.
- [13] Katharina Grünberg et al. "Ethical and Privacy Aspects of Using Medical Image Data". In: May 2017, pp. 33–43. ISBN: 978-3-319-49642-9. DOI: 10.1007/978-3-319-49644-3\_3.
- [14] Angjoo Kanazawa et al. "End-to-End Recovery of Human Shape and Pose". In: *Proceedings of the IEEE Conference on Computer Vision and Pattern Recognition (CVPR)*. June 2018.
- [15] Jeff Orschell Kathy Gramling and Joshua Chernoff. *How E-Commerce Fits into Retail's Post-Pandemic Future*. May 2021. URL: <https://hbr.org/2021/05/how-e-commerce-fits-into-retails-post-pandemic-future>.
- [16] Matthew Loper et al. "SMPL: A Skinned Multi-Person Linear Model". In: *ACM Trans. Graph.* 34.6 (Oct. 2015). ISSN: 0730-0301. DOI: 10.1145/2816795.2818013. URL: <https://doi.org/10.1145/2816795.2818013>.
- [17] Jennifer McAdams. *The Growing Importance of Ecommerce During COVID-19 Benefits of Online Selling*. Aug. 2021. URL: <https://www.progress.com/blogs/the-growing-importance-of-ecommerce-in-a-post-covid-19-world>.
- [18] Ahmed A A Osman, Timo Bolkart, and Michael J. Black. "STAR: A Spare Trained Articulated Human Body Regressor". In: *European Conference on Computer Vision (ECCV)*. 2020. URL: <https://star.is.tue.mpg.de>.
- [19] Giada Pezzini. *Why physical stores are still vital for retail*. Feb. 2021. URL: <https://www.lsretail.com/resources/why-physical-stores-are-still-vital-for-retail>.
- [20] Michael Pratscher et al. "iOutside-in/i Anatomy Based Character Rigging". In: *Proceedings of the 2005 ACM SIGGRAPH/Eurographics Symposium on Computer Animation*. SCA '05. Los Angeles, California: Association for Computing Machinery, 2005, pp. 329–338. ISBN: 1595931988. DOI: 10.1145/1073368.1073415. URL: <https://doi.org/10.1145/1073368.1073415>.
- [21] Kevin Roose. *Here Come the Fake Videos, Too*. Mar. 2018. URL: <https://www.nytimes.com/2018/03/04/technology/fake-videos-deepfakes.html>.
- [22] Shunsuke Saito et al. "PIFuHD: Multi-Level Pixel-Aligned Implicit Function for High-Resolution 3D Human Digitization". In: *Proceedings of the IEEE Conference on Computer Vision and Pattern Recognition*. June 2020.
- [23] Marco Schreyer et al. "Adversarial Learning of Deepfakes in Accounting". In: *ArXiv abs/1910.03810* (2019).
- [24] Hyewon Seo and Nadia Magnenat-Thalmann. "An Automatic Modeling of Human Bodies from Sizing Parameters". In: *Proceedings of the 2003 Symposium on Interactive 3D Graphics*. I3D '03. Monterey, California: Association for Computing Machinery, 2003, pp. 19–26. ISBN: 1581136455. DOI: 10.1145/641480.641487. URL: <https://doi.org/10.1145/641480.641487>.
- [25] UNCTAD. "How COVID-19 triggered the digital and e-commerce turning point". In: <https://unctad.org/news/how-covid-19-triggered-digital-and-e-commerce-turning-point>, Mar. 2021.
- [26] Andreas Volz et al. "Automatic, Body Measurements Based Generation of Individual Avatars Using Highly Adjustable Linear Transformation". In: *Digital Human Modeling*. Ed. by Vincent G. Duffy. Berlin, Heidelberg: Springer Berlin Heidelberg, 2007, pp. 453–459. ISBN: 978-3-540-73321-8.
- [27] Jungdam Won and Jehee Lee. "Learning Body Shape Variation in Physics-Based Characters". In: *ACM Trans. Graph.* 38.6 (Nov. 2019). ISSN: 0730-0301. DOI: 10.1145/3355089.3356499. URL: <https://doi.org/10.1145/3355089.3356499>.
- [28] Stefanie Wuhler and Chang Shu. "Estimating 3D human shapes from measurements". In: *Machine Vision and Applications* 24.6 (Dec. 2012), pp. 1133–1147. ISSN: 1432-1769. DOI: 10.1007/s00138-012-0472-y. URL: <http://dx.doi.org/10.1007/s00138-012-0472-y>.
- [29] Yipin Yang et al. "Semantic Parametric Reshaping of Human Body Models". In: *2014 2nd International Conference on 3D Vision*. Vol. 2. 2014, pp. 41–48. DOI: 10.1109/3DV.2014.47.
- [30] Marian Zboraj. *Consumers Still Prefer In-Store Shopping*. May 2021. URL: <https://progressivegrocer.com/consumers-still-prefer-store-shopping>.
- [31] T. Zhang et al. "See Through Occlusions: Detailed Human Shape Estimation From A Single Image With Occlusions". In: *2020 IEEE International Conference on Image Processing (ICIP)*. 2020, pp. 2646–2650. DOI: 10.1109/ICIP40778.2020.9191283.
- [32] Hao Zhu et al. "Detailed Human Shape Estimation From a Single Image by Hierarchical Mesh Deformation". In: *Proceedings of the IEEE/CVF Conference on Computer Vision and Pattern Recognition (CVPR)*. June 2019.